Interfacial Phenomena and Heat Transfer, 5(2): 113–128 (2017)

COMPARABLE EFFECTS OF ADSORPTION AND LINE TENSION ON CONTACT ANGLE OF A NUCLEATED DROPLET ON A PARTIALLY WETTABLE SUBSTRATE

Dmitry V. Tatyanenko & Alexander K. Shchekin*

St. Petersburg State University, 7–9 Universitetskaya nab., St. Petersburg, 199034, Russia

*Address all correspondence to: Dmitry V. Tatyanenko, St. Petersburg State University, Department of Statistical Physics, 1 Ulyanovskaya ul., Peterhof, St. Petersburg, 198504, Russia,
E-mail: d.tatyanenko@spbu.ru

Original Manuscript Submitted: 1/24/2018; Final Draft Received: 3/2/2018

Thermodynamics of a small sessile droplet on a solid substrate is discussed with a focus on size dependence of its contact angle. An interface displacement (ID) model is employed to calculate profiles and contact angles of sessile droplets representing, in particular, critical droplets in nucleation on a partially wettable solid substrate. Line-tension and adsorption-related corrections to the contact angle cosine are found within the ID model and illustrated with numeric calculations for a short-range interface potential. The line tension and adsorption effects on the contact angle are shown to be comparable even in the first order in the contact line curvature. For smaller droplets, an intrinsic dependence of the line tension on the contact line curvature also becomes significant for the contact angle.

KEY WORDS: *heterogeneous nucleation, partial wetting, contact angle, line tension, adsorption*

1. INTRODUCTION

Heterogeneity of a system usually plays a key role in nucleation of new phase embryos in different systems, drastically lowering the degree of metastability necessary for active nucleation process. Small heterogeneities (ions, micro-, meso-, and macro-scopic solid particles, both soluble and insoluble, charged and uncharged, etc.) act as nucleation centers, facilitating formation of critical droplets with an activation barrier lower than in a homogeneous mother phase.

At complete wetting of a chemically homogeneous spherical solid particle by condensate, in the absence of electric charges, a new phase embryo appearing in a supersaturated vapor is formed by a thin concentric liquid film* of the condensate around the particle surface (see Kuni et al., 2001, 1996).

At partial wetting of a solid surface, however, small sessile droplets of condensate are formed by nucleation on the surface of solid particles or substrates (Checco et al., 2003; Derjaguin and Zorin, 1955). If specific properties of thin liquid films are described with a disjoining pressure isotherm $\Pi(h)$, the appearance of sessile droplets is associated with loss of stability of a wetting film† in a thickness h range, where $\Pi'(h) > 0$ (Derjaguin et al., 1987) with forming of "humps". Being grown up, such local "humps" have spherical-segment shape, forming a contact angle with the surface of the solid. The fact that bulk liquid can form a contact angle with a polymolecular (adsorption or wetting) film is long known. Even though the disjoining pressure has been initially defined and measured for planar films, the disjoining-pressure-based approach to describing non-uniform in thickness films (and, in particular, a transition zone between a thin wetting film and a macroscopic meniscus/droplet) is widely used in theory of wetting.

*A film of non-uniform thickness is formed, in particular, in a case of heterogeneity of the solid particle itself. It can be a local chemical or structural heterogeneity/defect or a asymmetrically located (e.g., adsorbed) electric charge [see, e.g., Warshavsky et al. (2013a,b)].

†See Ajaev (2013) for detailed consideration of various instabilities of thin liquid films on solid substrates.

2169–2785/17/$35.00 www.begellhouse.com DOI: 10.1615/InterfacPhenomHeatTransfer.2018025483

General thermodynamic approach to description of sessile drops is often extrapolated down to very small critical droplets at nucleation. Such a description can be exact within Gibbs' method of dividing surfaces. However, it generally implies dependences of surface excesses (including surface tensions/energies) on chemical potentials of components' molecules of the system and curvatures of the dividing surfaces. It also takes into account line excesses, including the line tension/energy and its dependence on the chemical potentials and the contact line curvature (Rusanov, 2005; Rusanov et al., 2004). Most of the mentioned dependences are generally unknown.

Making simplifying assumptions, it is possible to find, within such a general thermodynamic approach, the work of droplet formation as a function of the radius of the droplet's free surface and/or contact line, the contact angle, the chemical potential(s) with taking into account the surface and, generally, the line tension. Thermodynamic theory of nucleation on flat and spherical solid surfaces was formulated within assumption of constant surface tensions without the line tension (Fletcher, 1958; Volmer, 1939) as well as with account of [constant] line tension (Gretz, 1966a,b; Iwamatsu, 2015a,b; Navascués and Tarazona, 1981; Radoev et al., 1986; Scheludko, 1980, 1983, 1985; Singha et al., 2015). The effect of the line tension on the contact angle and work of formation of very small (nanosized) droplets in the latter theories tends to appear a maximum on the dependence of the condensate molecules' chemical potential on the droplet size and, therefore, existence of a *threshold vapor supersaturation* above which the activation barrier to nucleation vanishes. Note that this maximum appears even in nucleation on a flat partially wettable substrate due to size dependence of the contact angle as a result of the line-tension effect. Existence of such a maximum is a hallmark of heterogeneous nucleation.

Since critical droplets in nucleation on a partially wettable surface are extremely small, applicability of such simplified descriptions is doubtful. Contact angles and even profiles of sub-micrometer sessile droplets can be measured using not only optical but also modern scanning-microscopy techniques, including atomic-force microscopy (Herminghaus et al., 2000; Seemann et al., 2001). Such measurements not only reveal the structure of the three-phase contact area but also demonstrate a non-linear dependence of the contact angle cosine on the contact line curvature (for nucleated nanosized alkane droplets on silanized silicon wafers, see Checco et al., 2003) in contrast to linear dependence used in simplified theories down to almost nanosized drops.

In the present work, we employ a local interface displacement (ID) model based on use of an effective interface potential (related to disjoining pressure isotherm) to find the profiles of sessile droplets—critical droplets at nucleation in a one-component supersaturated vapor on a flat partially wettable solid substrate. Such droplets are formed on top of a precursor film representing the equilibrium state of the solid surface in contact with the vapor. That is one of the possible nucleation scenarios near a wall/substrate (see Dash, 1977) and was directly observed and studied, e.g., for polar fluids (water and alcohols) on glass (Derjaguin and Zorin, 1955). Within the ID model, we calculate dependences of the solid–vapor surface tension on the chemical potential of molecules of the fluid (vapor/condensate) due to adsorption. We also calculate the size-dependent line tension of small droplets. Since the droplets profiles are known, we compare different size-related corrections to the contact angle cosine and demonstrate that they are comparable for small droplets. Moreover, the line-tension and adsorption effects on the contact angle give comparable corrections even in the first order in the contact line curvature. We present thermodynamic arguments and confirm them within the model, illustrating with numeric calculations for a representative interface potential.

The work has the following structure. In Section 2, a general thermodynamic description of a sessile droplet is given with a focus on size dependence of the contact angle. In Section 3, a local ID model is introduced, stationary profiles (corresponding to metastable state of the surface and a critical droplet) are discussed, including the context of nucleation; an expression for the adsorption-related correction to the contact angle cosine is derived. In Section 4, correspondence between general thermodynamic and ID descriptions of a sessile droplet is used to find an expression for the size-dependent line tension. Results of numeric calculations for three separate corrections to the contact angle cosine are presented in Section 5 and then discussed in Section 6.

2. THERMODYNAMICS OF A SESSILE DROPLET

Let us consider a materially open system of a fixed volume, including a solid substrate (phase γ), vapor (phase β) and a sessile droplet of the condensate (the bulk condensate phase will be referred to as α), forming a contact angle θ with the substrate surface. To simplify our consideration, let the fluid part of the system be one-component. Then,

within the general thermodynamic approach, the grand thermodynamic potential of the system decomposes into bulk, surface, and line contributions:

$$\Omega = \Omega^{\gamma} - p^{\beta}V^{\beta} - p^{\alpha}V^{\alpha} + \sigma^{\alpha\beta}A^{\alpha\beta} + \sigma^{\alpha\gamma}A^{\alpha\gamma} + \sigma^{\beta\gamma}A^{\beta\gamma} + \kappa L^{\alpha\beta\gamma}, \tag{1}$$

where V is the volume occupied by the corresponding phase, A is the area of the interface surface, p is the pressure in the corresponding *bulk* phase, σ is the thermodynamic surface tension, also known as the surface energy—the specific (i.e., per unit area) surface excess of the grand thermodynamic potential[‡]; single Greek superscripts mark the phase, double Greek superscripts mark the interfaces; Ω^{γ} is the grand thermodynamic potential of the bulk solid phase (see Rusanov et al., 2009), $L^{\alpha\beta\gamma}$ is the length of the three-phase contact line—the perimeter of the sessile droplet, κ is the thermodynamic line tension—the specific (i.e., per unit length) line excess of the grand thermodynamic potential.

Supposing the equilibrium droplet to have the shape of a spherical segment with the curvature radius R, the radius of the contact line r and the contact angle θ (see Fig. 1), one can easily write the expressions for the volume V^{α}, the areas $A^{\alpha\beta}$ and $A^{\alpha\gamma}$, the length $L^{\alpha\beta\gamma}$:

$$V^{\alpha} = \frac{1}{3}\pi R^3(2+\cos\theta)(1-\cos\theta)^2, \tag{2}$$

$$A^{\alpha\beta} = 2\pi R^2(1-\cos\theta), \quad A^{\alpha\gamma} = \pi R^2\sin^2\theta, \tag{3}$$

$$L^{\alpha\beta\gamma} = 2\pi r = 2\pi R\sin\theta, \quad \text{since} \quad r = R\sin\theta. \tag{4}$$

For the quantities V^{β} and $A^{\beta\gamma}$, one can write

$$V^{\beta} = V_{\mathrm{t}} - V^{\alpha}, \quad A^{\beta\gamma} = A_{\mathrm{t}} - A^{\alpha\gamma}, \tag{5}$$

where V_{t} is the total volume of the fluid (liquid–vapor) part of the system, A_{t} is the total substrate area (the joint area of the substrate/liquid, $\alpha\gamma$, and substrate/vapor, $\beta\gamma$, surfaces).

The excess quantities σ and κ standing in Eq. (1) are defined for chosen Gibbs dividing surfaces (spherical for $\alpha\beta$ surface and planar for $\alpha\gamma$ and $\beta\gamma$ surfaces. Putting Eqs. (2)–(5) into the right-hand side of Eq. (1) yields an expression for Ω in terms of R and θ:

$$\begin{aligned}\Omega(R,\theta) = &-\frac{1}{3}\pi R^3(p^{\alpha}-p^{\beta})(2+\cos\theta)(1-\cos\theta)^2 + 2\pi\sigma^{\alpha\beta}R^2(1-\cos\theta)\\ &-(\sigma^{\beta\gamma}-\sigma^{\alpha\gamma})\pi R^2\sin^2\theta + 2\pi\kappa R\sin\theta - p^{\beta}V_{\mathrm{t}} + \sigma^{\beta\gamma}A_{\mathrm{t}} + \Omega^{\gamma}.\end{aligned} \tag{6}$$

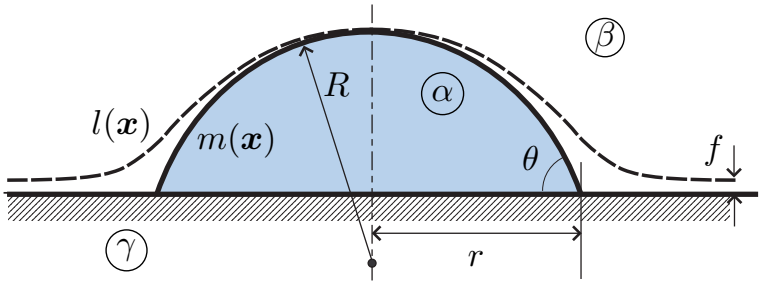

FIG. 1: Solid line: Schematic representation of a sessile droplet on a solid substrate. Circled Greek symbols mark phases: α is the liquid (colored), β is the vapor, γ is the solid substrate (striped). R is the curvature radius of $\alpha\beta$ surface, θ is the contact angle, r is the radius of the three-phase-contact line. Dashed line schematically represents an interface displacement profile $l(\boldsymbol{x})$ corresponding to the sessile droplet (see Section 3), $m(\boldsymbol{x})$ then denotes the reference profile (28).

[‡]See (Rusanov et al., 2009, 2010) for exact meaning of the quantity σ for solids and its difference from the mechanical surface tension, also known as the surface stress.

If the surface of tension is chosen as the $\alpha\beta$ dividing surface, equilibrium conditions

$$\partial\Omega/\partial R = 0, \quad \partial\Omega/\partial\theta = 0 \tag{7}$$

will give (Rusanov et al., 2004) the Laplace formula

$$p^{\alpha} - p^{\beta} = 2\sigma^{\alpha\beta}/R \tag{8}$$

and the generalized Young equation

$$\sigma^{\alpha\beta}\cos\theta = \sigma^{\beta\gamma} - \sigma^{\alpha\gamma} - \kappa/r - \partial\kappa/\partial r \tag{9}$$

as equations for equilibrium contact angle θ and radii R and r.

Note that Ω in Eqs. (1) and (6), as well as the quantities p^{α}, p^{β}, $\sigma^{\alpha\beta}$, $\sigma^{\alpha\gamma}$, $\sigma^{\beta\gamma}$, κ and $\partial\kappa/\partial r$ are taken at given values of the temperature T and the chemical potential μ (of molecules of the vapor/condensate)[§]. In this work, the system is supposed to be isothermal.

For a large (in the limit of infinite) droplet corresponding to the bulk liquid–vapor phase coexistence, i.e., the binodal, the generalized Young equation turns into the "classical" Young relation

$$\sigma_0^{\alpha\beta}\cos\theta_0 = \sigma_0^{\beta\gamma} - \sigma_0^{\alpha\gamma}, \tag{10}$$

where the subscript "0" refers to the thermodynamic state $\mu = \mu_0$ at the binodal.

Subtracting Eq. (9) from the Young relation (10) we arrive at

$$\sigma_0^{\alpha\beta}\cos\theta_0 - \sigma^{\alpha\beta}\cos\theta = \delta\Delta\sigma^{\gamma} + \kappa/r + \partial\kappa/\partial r, \tag{11}$$

where we have introduced

$$\delta\Delta\sigma^{\gamma} \equiv \Delta\sigma^{\gamma} - \Delta\sigma_0^{\gamma}, \quad \Delta\sigma^{\gamma} \equiv \sigma^{\alpha\gamma} - \sigma^{\beta\gamma}, \quad \Delta\sigma_0^{\gamma} \equiv \sigma_0^{\alpha\gamma} - \sigma_0^{\beta\gamma}. \tag{12}$$

Here and further, δ denotes the difference of the value of a quantity with its value at the binodal (at $\mu = \mu_0$).

Equation (11) is exact, however, it includes quantities with dependences on the chemical potential μ; the line tension κ also depends on the equilibrium contact line radius r. Usually, these dependences are neglected (or just silently ignored) and Eq. (9) is used in a simplified form often referred to as the *modified* or sometimes *extended* Young equation

$$\sigma_0^{\alpha\beta}\cos\theta = \sigma_0^{\beta\gamma} - \sigma_0^{\alpha\gamma} - \kappa_0/r. \tag{13}$$

Being subtracted from the "classical" Young relation (10), it gives a simplified form of Eq. (11):

$$\sigma_0^{\alpha\beta}(\cos\theta_0 - \cos\theta) = \kappa_0/r. \tag{14}$$

We used here the subscripts "0" to refer to the values of σ and κ at the binodal as corresponding to large droplets.

Equation (14) has been widely used in measurements of the line tension from the slope of $\cos\theta$ vs. $1/r$ (see, e.g., Amirfazli et al., 1998, a recent review of Law et al., 2017 and references therein). Since the curvature radius R of the $\alpha\beta$ surface is usually much larger than the Tolman length, we will also suppose $\sigma^{\alpha\beta} = \sigma_0^{\alpha\beta}$ (see discussion in Section 6; for estimations of the Tolman length see, e.g., Bykov and Shchekin, 1999a,b).

To estimate the term $\delta\Delta\sigma^{\gamma}$ in Eq. (11), let us employ the generalized Gibbs adsorption equation for $\beta\gamma$ and $\alpha\gamma$ surfaces—the solid-surface counterpart of the conventional Gibbs adsorption equation. Following Rusanov (1978, 1996, 2005), one can write for each of the flat solid–fluid surfaces

$$\mathrm{d}\sigma = -\bar{s}\,\mathrm{d}T + \left(\hat{\gamma} - \sigma\hat{1}\right) : \left(\mathrm{d}\hat{e} - \mathrm{d}\hat{N}_{(j)}/N_{(j)}\right) - \sum_i \Gamma_{(i)}\,\mathrm{d}\mu_{(i)}, \tag{15}$$

[§]The thermodynamic state of the solid is considered to be fixed in all our considerations: its temperature always equals T, and the change of the chemical potential(s) of the component(s) of the solid is neglected. Thus, we will not consider the possible effects of excess stress in solid substrate underneath the droplet on the droplet's thermodynamics.

where $\bar{s}$ is the specific (per unit area) surface excess of entropy, $\hat{\gamma}$ is the mechanical surface tension (surface stress) tensor, $\hat{e}$ is the surface strain tensor, $\hat{N}_{(j)}$ is the mass displacement tensor of the immobile component j of solid, $N_{(j)} \equiv \operatorname{Tr} \hat{N}_{(j)}$ is the amount of matter (the number of atoms/molecules) of the immobile component j in the solid phase, $\Gamma_{(i)}$ is the adsorption of a mobile component i at the interface, $\mu_{(i)}$ is the chemical potential of the molecules of this component; colon denotes a biscalar product of tensors.

For a non-deformable solid (or solid at a fixed strain) of a constant mass (within the boundaries defined by the dividing surfaces) $\mathrm{d}\hat{e} = 0$, $\mathrm{d}\hat{N}_{(j)} = 0$, and Eq. (15) yields the conventional form (as for a fluid–fluid interface) of the Gibbs adsorption equation (Rusanov, 1996, 2005):

$$\mathrm{d}\sigma = -\bar{s}\,\mathrm{d}T - \sum_i \Gamma_{(i)}\,\mathrm{d}\mu_{(i)}. \tag{16}$$

Assuming the solid to contain no mobile components, neglecting deformation of the solid substrate by the sessile droplet (assuming the strain of the solid to be independent of the droplet size and the chemical potential(s) of the fluid) and setting the $\beta\gamma$ and $\alpha\gamma$ dividing surfaces as equimolecular with respect to the immobile component j of the solid,¶ we apply Eq. (16) to both $\sigma^{\beta\gamma}$ and $\sigma^{\alpha\gamma}$ in our system. At $T = \mathrm{const}$, for a one-component fluid this yields

$$\mathrm{d}\Delta\sigma^{\gamma} = \left(\Gamma^{\beta\gamma} - \Gamma^{\alpha\gamma}\right)\mathrm{d}\mu. \tag{17}$$

Integration of this equation from the binodal to the current thermodynamic state gives

$$\delta\Delta\sigma^{\gamma} = \int_{\mu_0}^{\mu} \left(\Gamma^{\beta\gamma} - \Gamma^{\alpha\gamma}\right)\mathrm{d}\mu' \simeq \left(\Gamma_0^{\beta\gamma} - \Gamma_0^{\alpha\gamma}\right)\delta\mu, \quad \text{where} \quad \delta\mu \equiv \mu - \mu_0. \tag{18}$$

The latter is the asymptotic expression for large droplets. The subscript "0", as usual, refers to the thermodynamic state $\mu = \mu_0$ at the binodal.

To compare this result for $\delta\Delta\sigma^{\gamma}$ with κ/r, let us consider the Gibbs–Duhem equation

$$\mathrm{d}p = s\,\mathrm{d}T + n\,\mathrm{d}\mu \tag{19}$$

at a constant temperature for our one-component fluid for both α and β phases. Here s is the entropy density, n is the number density of molecules. Far from the critical point, the liquid (phase α) is almost incompressible and $n^{\beta} \ll n^{\alpha}$, and one can easily obtain by integration of Eq. (19) for α and β phases

$$p^{\alpha} - p^{\beta} \approx n^{\alpha}\delta\mu. \tag{20}$$

Comparing this with the Laplace formula (8) and the geometric relation $r = R\sin\theta$, one can obtain

$$r \approx \frac{2\sigma^{\alpha\beta}\sin\theta}{n^{\alpha}\delta\mu} \simeq \frac{2\sigma_0^{\alpha\beta}\sin\theta_0}{n^{\alpha}\delta\mu}, \tag{21}$$

which yields

$$\frac{\kappa}{r} \approx \frac{\kappa n^{\alpha}\delta\mu}{2\sigma^{\alpha\beta}\sin\theta} \simeq \frac{\kappa_0 n^{\alpha}\delta\mu}{2\sigma_0^{\alpha\beta}\sin\theta_0}. \tag{22}$$

The last expressions in Eqs. (21) and (22) are the asymptotic ones for large droplets.

Now one can see that the terms $\delta\Delta\sigma^{\gamma}$ and κ/r on the right-hand side of the Eq. (11) are of the same order in $\delta\mu$. As for the term $\partial\kappa/\partial r$, it can be estimated as $\mathcal{O}\left(r^{-2}\right)$, i.e., $\mathcal{O}\left((\delta\mu)^2\right)$, [see Rusanov (2005); Rusanov et al. (2004)]. Thus the simplified equation (14) is not correct. It can be technically considered as an asymptotic form of the exact equation (11) at $r \to \infty$, but with the coefficient

$$\kappa_0 + 2\sigma_0^{\alpha\beta}\sin\theta_0\left(\Gamma_0^{\beta\gamma} - \Gamma_0^{\alpha\gamma}\right)/n^{\alpha} \tag{23}$$

¶This practically means the dividing surface located at the boundary of the solid substrate as it can be reasonably defined.

on its right-hand side instead of κ_0. The slope of $\cos\theta$ vs. $1/r$ measured in many experiments, therefore, equals

$$-\kappa_0/\sigma_0^{\alpha\beta} - 2\sin\theta_0\left(\Gamma_0^{\beta\gamma} - \Gamma_0^{\alpha\gamma}\right)/n^{\alpha}, \tag{24}$$

not $-\kappa_0/\sigma_0^{\alpha\beta}$, as it is usually believed.

To compare the absolute values of $\delta\Delta\sigma^{\gamma}$ and κ/r and/or the terms in the sum (23), one has to measure them (or, one of them and the slope of $\cos\theta$ vs. $1/r$) independently or calculate them within a model. Since the simplified Eq. (14) is widely used to describe even nanoscale sessile droplets, it is also interesting to examine if all the three terms on the right-hand side of Eq. (11) are important for very small droplet sizes, where the first order (in $\delta\mu$ or $1/r$) approximation is not accurate enough.

As an example, we will consider critical droplets at nucleation on a partially wettable substrate. Such droplets are very small; however, the approximate Eq. (14) had been used to incorporate the line tension effect into the "classical" nucleation theory in the past (Gretz, 1966a,b; Navascués and Tarazona, 1981; Radoev et al., 1986; Scheludko, 1980, 1983, 1985) and still used in recent publications (e.g., Iwamatsu, 2015a,b; Singha et al., 2015).

In the next sections, we describe a local interface displacement model of a sessile droplet on a flat solid substrate and apply it to calculate $\delta\Delta\sigma^{\gamma}$, κ/r and $\partial\kappa/\partial r$. Since the term $\delta\Delta\sigma^{\gamma}$ is determined by the adsorptions [see Eq. (18)], we will refer to its effect on the contact angle as the effect of adsorption, while the effect of the term κ/r is usually referred to as the line-tension effect. The smaller (for large enough droplets) effect of the term $\partial\kappa/\partial r$ should also be included in the effect of the line tension, but can be called by itself, e.g., *the size-dependence effect of the line tension*.

3. INTERFACE DISPLACEMENT MODEL OF THE SYSTEM

Equations (8) and (9) of macroscopic capillarity and wetting contain quantities $p^{\alpha,\beta}(T,\mu)$, $\sigma^{\alpha\gamma,\beta\gamma,\alpha\beta}(T,\mu)$ and $\kappa(T,\mu,r)$ that must be known functions of their variables. To find the line and surface tensions as functions of corresponding variables, we employ a local interface displacement model widely used in the theory of wetting. Within the model, the liquid is represented with a film of varying thickness covering the surface of the substrate in the presence of another fluid (the vapor phase in our case). The solid substrate is assumed to be a rigid impenetrable wall interacting with the liquid–vapor interface with a known local *interface potential*.

The normal density distribution in the fluid phases is assumed to be sharp kink (see, e.g., Getta and Dietrich, 1998), i.e., the density is supposed to be constant within each fluid and equal to its bulk value at the same T and μ and abruptly change at the interfaces. Both solid–liquid and liquid–vapor interfaces are supposed to posses *interfacial tensions*. Due to the sharp-kink density distribution, there are no surface excesses of matter at the liquid–solid and liquid–vapor interfaces. According to the Gibbs adsorption equation (16), it means that the corresponding interfacial tensions will not depend on the chemical potentials. The values of the appropriate thermodynamic surface tensions $\sigma_0^{\alpha\gamma}$ and $\sigma_0^{\alpha\beta}$ at the bulk phase coexistence point $\mu = \mu_0$ will be used[‖]. The value $\sigma_0^{\alpha\gamma}$ corresponds to the surface tension of the $\alpha\gamma$ surface with the dividing surface located just at the solid wall and, therefore, can be considered as equimolecular with respect to the immobile component of the solid.

The state of the system is described by a liquid–vapor interface diplacement (i.e., variable film thickness) profile $l(\boldsymbol{x})$ with $\boldsymbol{x}$ the radius vector of a point on the substrate surface (see Fig. 1). The interface potential $U(l)$ includes all thin-film-specific contributions to the free energy (de Gennes, 1985; Dietrich, 1988; Dobbs and Indekeu, 1993; Indekeu, 1992) and can be expressed in terms of the disjoining pressure (Derjaguin et al., 1987) isotherm $\Pi(l)$ as $U(l) = \int_l^{\infty}\Pi(h)\,\mathrm{d}h$. Under assumption of incompressibility of the liquid, the grand thermodynamic potential of the system takes form (Dobbs and Indekeu, 1993)

$$\Omega^{(\mathrm{ID})}[l(\boldsymbol{x});T,\mu] = \Omega^{\gamma} - p^{\beta}V_{\mathrm{t}} + \int\left[\sigma_0^{\alpha\gamma} + \sigma_0^{\alpha\beta}\sqrt{1+(\nabla l)^2} + U(l(\boldsymbol{x})) - n^{\alpha}\delta\mu\, l(\boldsymbol{x})\right]\mathrm{d}^2\boldsymbol{x}, \tag{25}$$

[‖] We intentionally make terminological difference: the *interfacial tensions* are surface excesses of the grand thermodynamic potential referred to the interfaces of the film *within the model*, while the *surface tensions* are the surface excesses referred to dividing surfaces between macroscopic phases. The former are parameters of the model, the latter appear in thermodynamic description (see Section 2) and can vary depending on choice of dividing surfaces, even being applied to the same model system.

integration is to be done over the whole substrate surface. This expression defines $\Omega^{(\mathrm{ID})}$ as a functional with respect to the ID profile $l(\boldsymbol{x})$ and a function with respect to thermodynamic variables T and μ.

Assuming axial symmetry, one can rewrite the functional Eq. (25) in polar coordinates:

$$\Omega^{(\mathrm{ID})}[l(x);T,\mu] = \Omega^{\gamma} - p^{\beta}V_{\mathrm{t}} + \sigma^{\beta\gamma}\pi x_{\max}^2 + 2\pi\int_0^{x_{\max}} \left[\Delta\sigma^{\gamma} + \sigma_0^{\alpha\beta}\sqrt{1+l_x^2} + U(l(x)) - n^{\alpha}\delta\mu\, l(x)\right] x\ \mathrm{d}x, \quad (26)$$

where x is the radial coordinate, $\Delta\sigma^{\gamma} = \sigma_0^{\alpha\gamma} - \sigma^{\beta\gamma}$ [as defined in Eq. (12) with account of $\sigma^{\alpha\gamma} = \sigma_0^{\alpha\gamma}$ within the ID model]. Here we have chosen a circle of a large enough radius $x_{\max}$ as the domain of integration, meaning that the system is contained in a cylinder with radius $x_{\max}$, normal to the substrate surface. We can rewrite the thermodynamic expression (1) for Ω in a similar form as

$$\Omega[m(x);T,\mu] = \Omega^{\gamma} - p^{\beta}V_{\mathrm{t}} + \sigma^{\beta\gamma}\pi x_{\max}^2 + 2\pi\int_0^{r} \left[\Delta\sigma^{\gamma} + \sigma^{\alpha\beta}\sqrt{1+m_x^2} - n^{\alpha}\delta\mu\, m(x)\right] x\ \mathrm{d}x + 2\pi\kappa r, \quad (27)$$

where

$$m(x) \equiv \begin{cases} \sqrt{R^2-x^2} - R\cos\theta, & x < r \ (\text{while } m(x) > 0), \\ 0, & x \geq r \end{cases} \quad (28)$$

is the "macroscopic" spherical-segment-shaped profile of the sessile droplet forming a contact angle $\cos\theta$ with the substrate surface (see Fig. 1). Expression (27) can be considered as a functional of $m(x)$ which stationary profile (28) can be obtained together with Eqs. (8) and (9) [taking into account Eq. (20)], using a transversal boundary condition at $m(x) = 0$ (see Marmur, 1998; Rusanov, 1977, 1996).

The Euler–Lagrange equation of the functional Eq. (26) is

$$-\sigma_0^{\alpha\beta}\left(\frac{\mathrm{d}}{\mathrm{d}x} + \frac{1}{x}\right)\frac{l_x}{\sqrt{1+l_x^2}} - \Pi(l(x)) = n^{\alpha}\delta\mu. \quad (29)$$

The first term on the left-hand side of this equation is the local capillary pressure [the local mean curvature of the $l(\boldsymbol{x})$ interface multiplied by $-\sigma_0^{\alpha\beta}$]. The second term is the local disjoining pressure taken with the opposite sign. Since it has been initially defined, measured and calculated for planar films uniform in thickness, using it within this model implies at least smooth non-uniformity, i.e., $l_x \ll 1$. For large interface displacements (film thicknesses), $\Pi(l)$ becomes negligible and Eq. (29) turns into equation of a constant mean curvature.

Typical shapes of the interface potential isotherm $U(l)$ are represented in Figs. 2(a) and 2(b). The local minimum (and a zero of the disjoining pressure) at f_0 corresponds to the equilibrium film thickness at bulk phase coexistence.

We have numerically calculated stationary profiles [solutions of Eq. (29)] for several different interface potentials of typical shapes (see an example in Section 5). We have applied boundary conditions

$$l_x(0) = 0, \qquad l_x \xrightarrow[x\to\infty]{} 0 \quad (30)$$

by realizing a Runge–Kutta shooting method. We chose an initial interface displacement $l(0)$, solved numerically an initial value problem with $l_x(0) = 0$ and searched for appropriate value(s) of $\delta\mu$ to satisfy the boundary condition at $x \to \infty$ (technically, at a finite, sufficiently large value $x_{\max}$, in order to regularize the problem).

In all the cases, we have found two solutions at $0 < \delta\mu < -\Pi(f_{\mathrm{us}})/n^{\alpha}$ (see Fig. 2 for notations and schematic representation of the solutions) and no solutions at larger $\delta\mu$. The first, trivial, solution is a film of a constant thickness f that can be easily found by setting to zero the first (curvature) term on the left-hand side of Eq. (29):

$$-\Pi(f) = n^{\alpha}\delta\mu. \quad (31)$$

This is a non-linear algebraic equation. We need to choose solution(s) corresponding to [meta]stable film(s), i.e., delivering a weak minimum to the functional Eq. (26). Using direct analysis of the second variation (Mechkov et al., 2007) or appropriate conditions of variational calculus (Churaev et al., 1982), it can be shown, that this requires

$$\Pi'(f) \equiv \mathrm{d}\Pi(f)/\,\mathrm{d}f < 0. \quad (32)$$

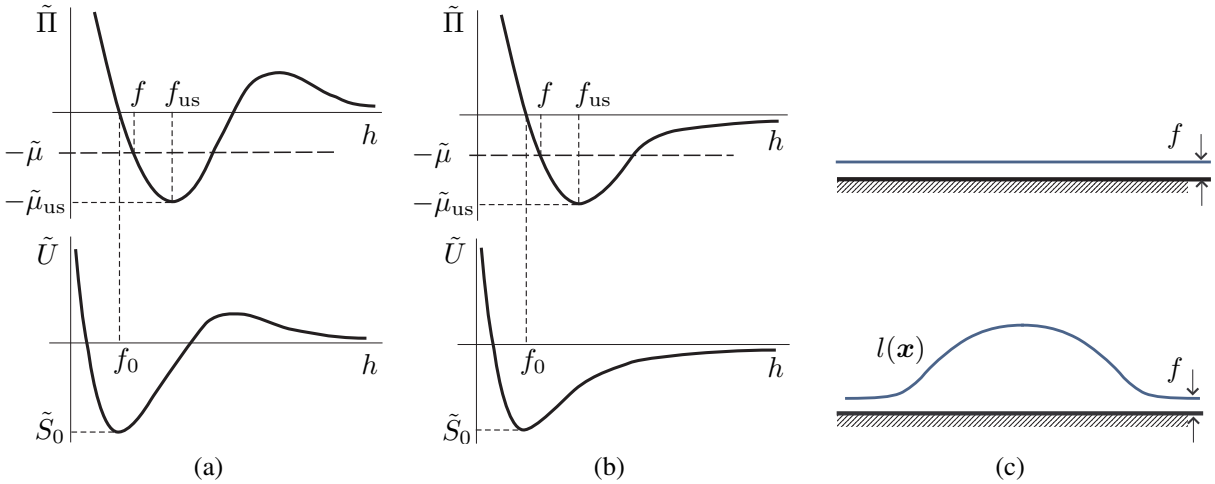

FIG. 2: (a) and (b) Schematic representation of typical shapes of disjoining pressure isotherms $\Pi(h)$ and corresponding interface potentials $U(h) = \int_h^\infty \Pi(h')\,\mathrm{d}h'$ for a partially wettable substrate. The graphs are labeled with "reduced" quantities $\tilde{\Pi} \equiv \Pi/\sigma_0^{\alpha\beta}$, $\tilde{U} \equiv U/\sigma_0^{\alpha\beta}$, $\tilde{S}_0 \equiv S_0/\sigma_0^{\alpha\beta}$, $\tilde{\mu} \equiv \delta\mu/(n^\alpha\sigma_0^{\alpha\beta})$ and corresponding $\tilde{\mu}_{\rm us} \equiv \delta\mu_{\rm us}/(n^\alpha\sigma_0^{\alpha\beta})$ that will be used later in the text. (c) Two solutions [trivial, corresponding to Eq. (31), and non-trivial] of the boundary problem (30) for the Eurler–Lagrange Eq. (29).

For supersaturated vapor ($\delta\mu > 0$), this condition is fulfilled in a limited range of film thicknesses $f_0 < f < f_{\rm us}$, usually lying within $\sim 10^{-1}$–10^1 nm. The lower limit corresponds to $\delta\mu \to +0$, i.e., the binodal. The upper limit corresponds to the (negative) minimum of $\Pi(f)$ and sets the upper limit $\delta\mu_{\rm us}$ of existence of metastable films. The set of such limiting states at different T and μ is often referred to as the *upper surface spinodal* (see Indekeu and Bonn, 1995, 1997; Nakanishi and Pincus, 1983) which is indicated with "us" subscripts in our notation.

The second, non-trivial, solution is a "hump" on top of the film of thickness f. The smaller the value of (positive) $\delta\mu$, the higher the "hump" is. At small values of $\delta\mu$, the "hump" clearly represents the sessile droplet with a large top part lying out of the range of surface forces and, therefore, with spherical-segment-shaped surface with curvature radius $R = 2\sigma_0^{\alpha\beta}\left(n^\alpha\delta\mu\right)^{-1} = 2\sigma_0^{\alpha\beta}\left(p^\alpha - p^\beta\right)^{-1}$ in accordance with the Laplace formula (8). At higher values of $\delta\mu$, the height of the "hump" decreases and, finally, $l(0) \to f_{\rm us} + 0$ together with $f \to f_{\rm us} - 0$ at $\delta\mu \to \delta\mu_{\rm us} - 0$. This means that the first and the second solutions merge at the upper surface spinodal. Using direct analysis of the second variation (Mechkov et al., 2007, see also Blossey and Bausch, 1994), it can be shown, that the second solution delivers a "saddle point" to the functional (26) with the only unstable growth–evaporation mode, i.e., represents the critical droplet at nucleation.

The underlying film of thickness f, therefore, shows that the first, trivial, solution gives us a precursor metastable film which is initially formed on the surface of the substrate in the presence of vapor and represents the equilibrium (strictly speaking, metastable) state of the surface. Later, liquid phase embryos nucleate and grow on this precursor film. This corresponds to direct observations (see, e.g., Derjaguin et al., 1987; Derjaguin and Zorin, 1955). The grand thermodynamic potential of our system with this equilibrium $\beta\gamma$ surface in absence of droplets can be expressed within general thermodynamic description (27) and within the ID model (26), giving the same result:

$$\Omega^\gamma - p^\beta V_{\rm t} + \sigma^{\beta\gamma} A_{\rm t} = \Omega^\gamma - p^\beta V_{\rm t} + \left(\sigma_0^{\alpha\gamma} + \sigma_0^{\alpha\beta} + U(f) - n^\alpha\delta\mu f\right) A_{\rm t}. \tag{33}$$

This gives us the following relation between the equilibrium values of thermodynamic surface tensions:

$$\Delta\sigma^\gamma \equiv \sigma^{\alpha\gamma} - \sigma^{\beta\gamma} = \sigma_0^{\alpha\gamma} - \sigma^{\beta\gamma} = n^\alpha\delta\mu f - U(f) - \sigma_0^{\alpha\beta}. \tag{34}$$

In the limit $\delta\mu \to +0$, Eq. (34) gives

$$\Delta\sigma_0^\gamma \equiv \sigma_0^{\alpha\gamma} - \sigma_0^{\beta\gamma} = -U(f_0) - \sigma_0^{\alpha\beta}. \tag{35}$$

This, in particular, leads to an expression for the *spreading coefficient* within the ID model

$$S_0 \equiv \sigma_0^{\beta\gamma} - \sigma_0^{\alpha\gamma} - \sigma_0^{\alpha\beta} = \sigma_0^{\alpha\beta}(\cos\theta_0 - 1) = U(f_0) \tag{36}$$

and an expression for $\delta\Delta\sigma^{\gamma}$:

$$\delta\Delta\sigma^{\gamma} \equiv \Delta\sigma^{\gamma} - \Delta\sigma_0^{\gamma} = n^{\alpha}\delta\mu f + U(f_0) - U(f). \tag{37}$$

For large enough sessile droplets (small values of $\delta\mu$), the thickness f of the underlying film can be approximately expressed from Eq. (31) applied at the current value of $\delta\mu$ and at $\delta\mu = 0$:

$$n^{\alpha}\delta\mu = \Pi(f_0) - \Pi(f) \simeq -\Pi'(f_0)(f - f_0). \tag{38}$$

Therefore, $f - f_0 \simeq -n^{\alpha}\delta\mu/\Pi'(f_0)$ [note, that $\Pi'(f_0) < 0$, cf. Eq. (32)] and, since $U'(f_0) = -\Pi(f_0) = 0$, one can obtain $U(f) - U(f_0) \simeq 1/2\, U''(f_0)(f - f_0)^2 = -1/2\,(n^{\alpha}\delta\mu)^2/\Pi'(f_0)$. Substituting the latter into Eq. (37), we arrive at

$$\delta\Delta\sigma^{\gamma} \simeq n^{\alpha}\delta\mu f + \frac{1}{2}(n^{\alpha}\delta\mu)^2/\Pi'(f_0) \simeq n^{\alpha}\delta\mu f_0. \tag{39}$$

Since, within the ID model and at chosen solid–fluid dividing surfaces, $\Gamma^{\alpha\gamma} = 0$ and $\Gamma^{\beta\gamma} = n^{\alpha}f$, Eq. (39) exactly reproduces Eq. (18). As a consequence, Eq. (24) for the slope of $\cos\theta$ vs. $1/r$ takes form

$$-\kappa_0/\sigma_0^{\alpha\beta} - 2f_0\sin\theta_0. \tag{40}$$

The activation barrier to nucleation of sessile droplets then equals

$$\delta\Omega^{(\mathrm{ID})}(T,\mu) = \Omega^{(\mathrm{ID})}[l(x);T,\mu] - \Omega^{(\mathrm{ID})}[f;T,\mu], \tag{41}$$

and the nucleation rate J is

$$J \propto \exp\left(-\frac{\delta\Omega^{(\mathrm{ID})}}{k_{\mathrm{B}}T}\right). \tag{42}$$

Expectedly, $\delta\Omega^{(\mathrm{ID})} \to 0$ at $\delta\mu \to \delta\mu_{\mathrm{us}} - 0$, i.e., the activation barrier to nucleation vanishes at the upper surface spinodal, and nucleation becomes barrierless (turning into what can be called "surface spinodal decomposition" at $\delta\mu > \delta\mu_{\mathrm{us}}$).

4. THREE-PHASE CONTACT LINE RADIUS, CONTACT ANGLE AND LINE TENSION

To find the contact angle θ, the radius r of the three-phase contact line and to calculate the line tension κ for a given interface displacement profile $l(x)$ found at specific values of T and μ, one should define a corresponding reference "macroscopic" profile $m(x)$ [see Eq. (28)]. The correspondence is set by the Laplace formula (8), which gives the value of R, and another condition to be specified by measurement procedure. Bearing in mind such methods as atomic force microscopy (AFM) that can give droplet profiles similar to $l(\boldsymbol{x})$ in our model, we consider the condition $m(0) = l(0)$ of profiles touching at their top (see Fig. 1) as the most natural. Then

$$m(x) \equiv \begin{cases} \sqrt{R^2 - x^2} - R + l(0), & x < r \text{ (while } m(x) > 0), \\ 0, & x \geq r, \end{cases} \tag{43}$$

r and θ can be found from

$$r = \sqrt{\big(2R - l(0)\big)\, l(0)}, \qquad \cos\theta = 1 - l(0)/R. \tag{44}$$

Then, the line tension κ can be calculated from the equation

$$\Omega^{(\mathrm{ID})}[l(x);T,\mu] = \Omega[m(x);T,\mu], \tag{45}$$

where the functionals are defined by Eqs. (26) and (27). This gives, with use of relation (34),

$$\kappa = \frac{1}{r}\left\{\int_0^\infty \left[\sigma_0^{\alpha\beta}\left(\sqrt{1+l_x^2}-1\right)+U(l(x))-U(f)-n^\alpha\delta\mu\left(l(x)-f\right)\right]x\,\mathrm{d}x\right.$$
$$\left.-\int_0^r\left[\sigma_0^{\alpha\beta}\left(\sqrt{1+m_x^2}-1\right)-U(f)-n^\alpha\delta\mu\left(m(x)-f\right)\right]x\,\mathrm{d}x\right\}. \quad (46)$$

Here we have replaced a formal upper limit of integration $x_{\max}$ with ∞ in the first of the integrals, since this integral already converge [in contrast to the integral in expression (26)]. Introducing a function

$$m_1(x) \equiv \begin{cases} m(x), & x < r, \\ f, & x \geq r, \end{cases} \quad (47)$$

we can rewrite expression (46) in a more compact form

$$\kappa = \frac{1}{r}\int_0^\infty \left[\sigma_0^{\alpha\beta}\left(\sqrt{1+l_x^2}-\sqrt{1+m_{1x}^2}\right)+U(l(x))-U(f)-n^\alpha\delta\mu\left(l(x)-m_1(x)\right)\right]x\,\mathrm{d}x+\frac{r}{2}U(f). \quad (48)$$

Even thought the non-integral term $rU(f)/2$ diverges at $\delta\mu \to +0$, it is compensated by $(1/r)\int_0^\infty \left[U(l(x))-U(f)\right]x\,\mathrm{d}x$, since for the most part of a large enough droplet, $U(l(x))$ is very small. The other terms under the integral substantially differ from zero at $\delta\mu \to +0$ only in the three-phase contact region. Therefore, they will give an integral contribution proportional to r, i.e., hopefully, a convergent contribution to κ.

To calculate the thermodynamic line tension κ_0 of an infinite droplet (i.e., of a straight contact line), one can calculate the expression (46) or (48) in the limit $\delta\mu \to +0$. It can be done numerically, but the same result can be obtained analytically for a straight contact line (Dobbs and Indekeu, 1993). In Cartesian coordinates, the Euler–Lagrange equation for a stationary interface displacement profile takes the form [cf. Eq. (29)]

$$\sigma_0^{\alpha\beta} l_{xx}\left(1+l_x^2\right)^{-3/2}+\Pi(l(x))=0, \quad (49)$$

with x the Cartesian coordinate along the change of the interface displacement (perpendicular to the contact line). The first integral of this equation is

$$\sigma_0^{\alpha\beta}\left(1+l_x^2\right)^{-1/2}=1-U(l(x))+U(f_0)=1-U(l(x))+S_0. \quad (50)$$

We used a boundary condition at a flat film asymptote $l(x) \to f_0$, $l_x \to 0$ (let it be at $x \to -\infty$). At the other limit $x \to \infty$, the profile forms a wedge with a slope $l_x = \tan\theta_0$. Then, using the "classical" Young relation (10), we obtain the latter of the equalities (50), reproducing the relation (36) in this geometry.

Substituting l_x from (50) into appropriate expression for $\Omega^{(\mathrm{ID})}[l(x)]$ and switching to interface displacement as an independent variable (Indekeu, 1992), one can obtain (Dobbs and Indekeu, 1993)

$$\tilde{\kappa}_0 = -f_0\sqrt{-\tilde{S}_0\left(2+\tilde{S}_0\right)}+\int_{f_0}^\infty\left[\sqrt{\left(\tilde{U}(h)-\tilde{S}_0\right)\left(2-\tilde{U}(h)+\tilde{S}_0\right)}-\sqrt{-\tilde{S}_0\left(2+\tilde{S}_0\right)}\right]\mathrm{d}h. \quad (51)$$

Here we used $\tilde{\kappa}_0 \equiv \kappa_0/\sigma_0^{\alpha\beta}$, $\tilde{U} \equiv U/\sigma_0^{\alpha\beta}$, $\tilde{S}_0 \equiv S_0/\sigma_0^{\alpha\beta}$. Note, that $\tilde{S}_0 = \cos\theta_0 - 1 < 0$. For small contact angles, $\tilde{U}(h) \ll 1$, and expression (51) turns into a simpler one (Indekeu, 1992):

$$\tilde{\kappa}_0 \simeq -f_0\sqrt{-2\tilde{S}_0}+\int_{f_0}^\infty\left[\sqrt{2\left(\tilde{U}(h)-\tilde{S}_0\right)}-\sqrt{-2\tilde{S}_0}\right]\mathrm{d}h. \quad (52)$$

The first, non-integral term in expressions (51) and (52) is absent in [Dobbs and Indekeu (1993) and Indekeu (1992)]. It is a contribution from a small fragment of the reference profile $m(x)$ located between the substrate surface

and the distance f_0 (underlying film thickness) from it. It does not appear in appropriate expressions in the above mentioned works, since the dividing plane between the solid substrate and the fluid phases has been set there at the distance f_0 from the substrate (i.e., on top of the underlying film). Such a consideration does make sense, especially in the vicinity of the upper surface spinodal ($\mu \to \mu_{us} - 0$), where nucleation actually occurs, and the height of [critical] droplets is comparable with the thickness f of the precursor/underlying film. However, consistent use of such dividing surfaces with solid bodies requires a more detailed analysis, in particular, of Eq. (15).

Since $\sqrt{-\tilde{S}_0\left(2+\tilde{S}_0\right)} = \sin\theta_0$, the first, non-integral term in expression (51) equals $-f_0 \sin\theta_0$. Then, the slope (40) of the curve $\cos\theta$ vs. $1/r$ equals

$$f_0\sqrt{-\tilde{S}_0\left(2+\tilde{S}_0\right)} + \int_{f_0}^{\infty}\left[\sqrt{\left(\tilde{U}(h)-\tilde{S}_0\right)\left(2-\tilde{U}(h)+\tilde{S}_0\right)} - \sqrt{-\tilde{S}_0\left(2+\tilde{S}_0\right)}\right]\mathrm{d}h. \tag{53}$$

5. CALCULATIONS FOR A MODEL INTERFACE POTENTIAL

To illustrate our theoretical results and to compare the effects of line tension and adsorption on the contact angle, we took a simple short-range potential, used by Dobbs (1999):

$$\tilde{U}(h) \equiv U(h)/\sigma_0^{\alpha\beta} = Ae^{-(h-1)} + Be^{-2(h-1)} + Ce^{-3(h-1)} \tag{54}$$

with $A = 3.3$, $B = -7.0$, $C = 3.5$ (see Fig. 3). With these parameters, $\tilde{S}_0 = -0.203$, $\theta_0 = 0.65$ rad, $f_0 = 0.97$, the upper surface spinodal is at $\tilde{\mu}_{us} = 0.970$, $f_{us} = 1.29$. It is convenient to use other "reduced" quantities as well:

$$\tilde{\kappa} \equiv \kappa/\sigma_0^{\alpha\beta}, \quad \Delta\tilde{\sigma}^{\gamma} \equiv \Delta\sigma^{\gamma}/\sigma_0^{\alpha\beta}, \quad \tilde{\mu} \equiv \delta\mu/\left(n^{\alpha}\sigma_0^{\alpha\beta}\right). \tag{55}$$

The line tension of a straight line for this potential, calculated from expression (51), equals $\tilde{\kappa}_0 = 0.22$. It is not only comparable with $2f_0 \sin\theta_0 = 1.17$, but notably less than it. This means that, for this particular potential, the effect of adsorption on the contact angle of [not very] small droplets is even more pronounced than the line tension effect. Figure 4 shows $\cos\theta$ vs. $1/r$, computed from Eq. (44), in wide range of droplet sizes, as well as asymptotic dependences according to the "simplified" modified Young equation (14) and similar asymptotic form with the correct slope (53). The slope of the curve $\cos\theta$ vs. $1/r$ clearly equals the quantity (53), a form of expressions (40) and (24) within the ID model, at $1/r \to 0$. However, it notably deviates from this asymptotic behavior at smaller droplets.

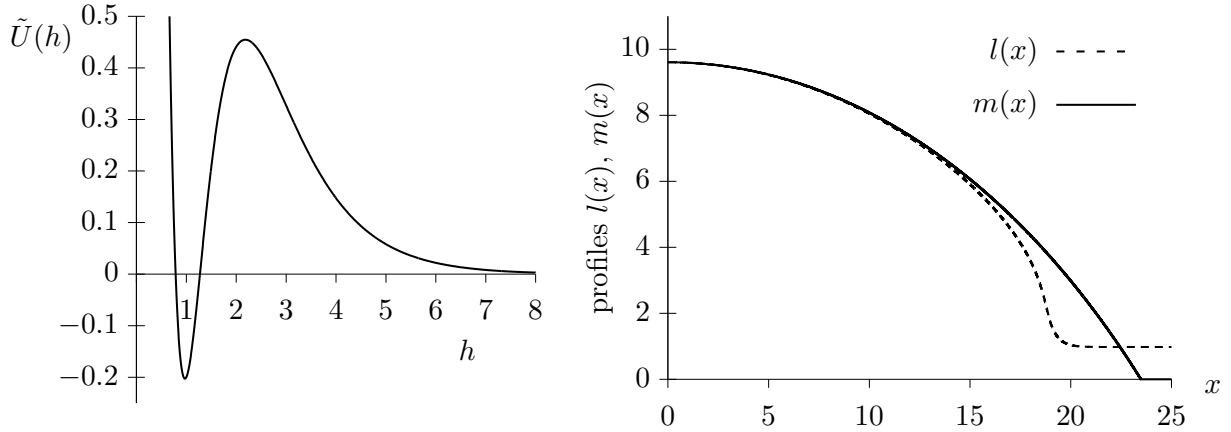

FIG. 3: Left: Model short-range "reduced" interface potential (54) with $A = 3.3$, $B = -7.0$, $C = 3.5$. Right: Calculated interface displacement profile $l(x)$ of the sessile droplet (dashed line) at $\tilde{\mu} = 0.060$ and corresponding "macroscopic" reference profile $m(x)$ (cf. schematic representation in Fig. 1). Interface displacement profile $l(x)$ lies below $m(x)$ due to presence of the positive disjoining pressure $\Pi(h) = -U'(h)$ branch at large values of film thickness h [see Eq. (29)].

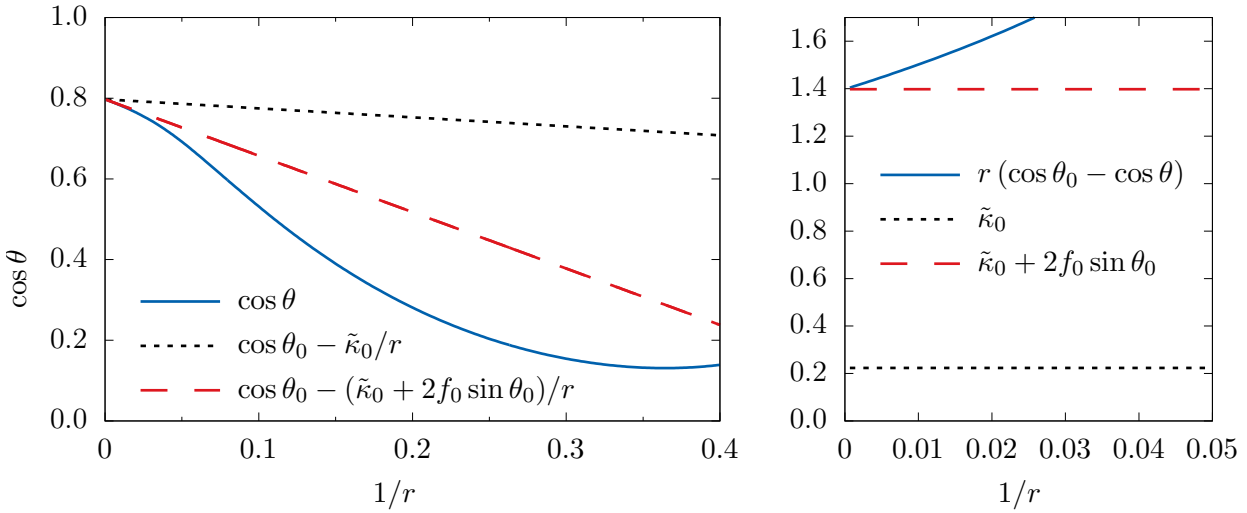

FIG. 4: Left: Calculated $\cos\theta$ vs. $1/r$ and corresponding asymptotic dependences according to the "simplified" modified Young Eq. (14) and similar asymptotic form with the correct slope (53), a form of expressions (40) and (24). Right: Calculated difference $(\cos\theta_0 - \cos\theta)$ and appropriate corrections to $\cos\theta_0$ according to both asymptotes, all multiplied by r, vs. $1/r$, close-up of the large-droplet range. Here it is clear that $-\tilde{\kappa}_0 - 2f_0\sin\theta_0$ indeed gives the correct slope of $\cos\theta$ vs. $1/r$ in $r \to \infty$ limit. Results from the ID model with the interface potential (54).

To compare the corrections to the contact angle cosine at different values of $\delta\mu$ (different droplet sizes), we have calculated κ/r using expression (48), $\delta\Delta\sigma^{\gamma}$ using expression (37), and $\partial\kappa/\partial r$ expressing it with use of Eqs. (11), (36) and (37) as

$$\partial\kappa/\partial r = \sigma_0^{\alpha\beta}(1-\cos\theta) + U(f) - n^{\alpha}\delta\mu f - \kappa/r, \tag{56}$$

or, for "reduced" quantities (54) and (55),

$$\partial\tilde{\kappa}/\partial r = 1 - \cos\theta + \tilde{U}(f) - \tilde{\mu}f - \tilde{\kappa}/r. \tag{57}$$

Results are presented in Fig. 5. It can be seen that all three corrections are comparable for small enough droplets. Even it is not clear from the main graph, $\tilde{\kappa}/r$ and $\delta\Delta\tilde{\sigma}^{\gamma}$ are indeed $\mathcal{O}(1/r)$, while $\partial\tilde{\kappa}/\partial r = \mathcal{O}(1/r^2)$. It can be seen on the close-up graph of the large-droplet range, where the corrections are multiplied by r. Another curious observation: relatively small (at $r \to \infty$) line-tension correction term $\tilde{\kappa}/r$ decreases with decrease of r and even changes its sign from positive to negative at smaller droplet sizes. That is, of course, not the common case.

6. DISCUSSION

As one can see, our results demonstrate that the line-tension effect on the contact angle is not the only significant effect even in the first order in the contact line curvature $1/r$ (or, the chemical potential shift $\delta\mu$ from the binodal). Thermodynamic arguments give that the adsorption-related correction to $\cos\theta_0$ is of the same order in $1/r$ (or $\delta\mu$), and calculations within the interface displacement model support it, showing that they can be of the same order in magnitude (and, the adsorption effect can be even more pronounced).

Within the interface displacement model, the line tension κ_0 of a straight line can be calculated analytically [see Eqs. (51) and (52) representing results of Dobbs and Indekeu (1993); Indekeu (1992)]. Its typical value can be estimated as $\kappa_0 \sim \sigma_0^{\alpha\beta}\xi$, with ξ the interface potential range, a typical length lying within the thickness range where the interface potential is substantially non-zero. As we saw at the end of Section 3, $\tilde{\kappa}_0 = \kappa_0/\sigma_0^{\alpha\beta} \sim \xi$ is to be compared with the adsorption-related contribution $2f_0\sin\theta_0$. The latter also lies within the same thickness range if the macroscopic contact angle θ_0 is not very small.

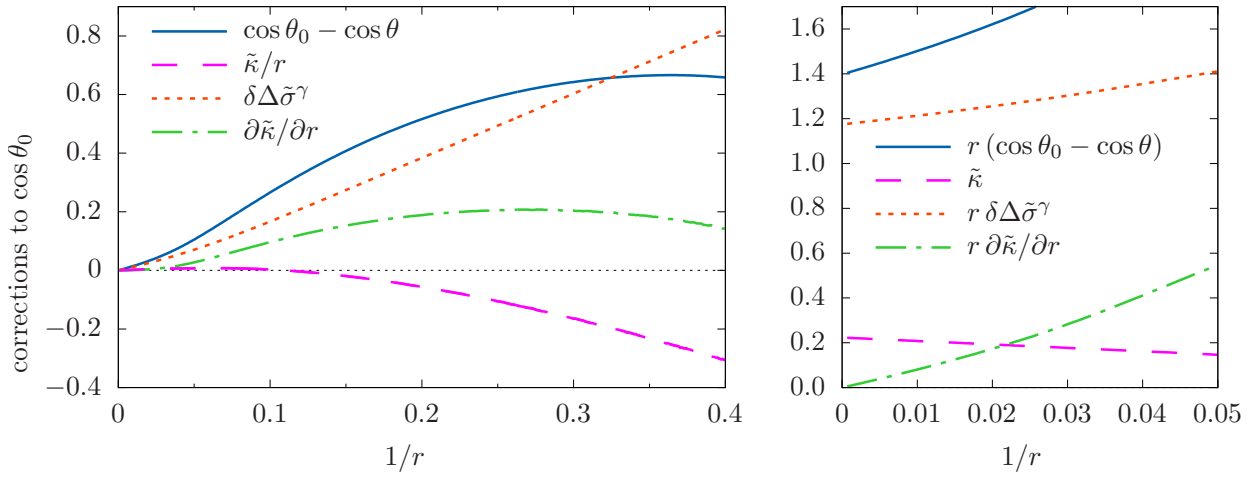

FIG. 5: Left: Separate correction terms to $\cos\theta_0$ in Eq. (11): $\tilde{\kappa}/r$, $\delta\Delta\tilde{\sigma}^\gamma$, $\partial\tilde{\kappa}/\partial r$, and the full difference $(\cos\theta_0 - \cos\theta)$ vs. the contact line curvature $1/r$, calculated within the ID model. Right: The same quantities multiplied by r, close-up of the large-droplet range. Here it is clear that $\tilde{\kappa}/r$ and $\delta\Delta\tilde{\sigma}^\gamma$ are $\mathcal{O}(1/r)$, while $\partial\tilde{\kappa}/\partial r = \mathcal{O}(1/r^2)$. The interface potential (54) is used.

The role of solid–fluid adsorptions in size dependence of the contact angle for small sessile droplets was pointed out earlier by Ward and Wu (2008). They have shown that the adsorption effect can be large enough to explain the size dependence of the contact angle even without the line tension. However, both contributions exist in real systems, and the model we have employed illustrates that they are inseparable and have joint effect.

For smaller droplets, the third correction to $\cos\theta_0$ becomes also significant—the term $\partial\kappa/\partial r$ appearing in the generalized Young Eq. (9) due to intrinsic contact-line-curvature dependence of the line tension. It also cannot be separated from other corrections in real system. This partial derivative should not be confused with full derivative $\mathrm{d}\kappa/\,\mathrm{d}r$ along the equilibrium/critical droplet sizes. While the partial derivative $\partial\kappa/\partial r$ is taken at fixed values of T and μ, the full derivative $\mathrm{d}\kappa/\,\mathrm{d}r$ corresponds to change of equilibrium values of r and κ at changing T and/or μ. In the isothermal case, e.g., it would correspond to calculation of changes $\mathrm{d}\kappa$ and $\mathrm{d}r$ of corresponding equilibrium values at a variation $\mathrm{d}\mu$ of the chemical potential. See Rusanov et al. (2004) for a more detailed explanation.

Ignoring size dependence of the line tension for very small droplets can give interesting predictions concerning small droplet morphology and wetting behavior (see, e.g., Lv et al., 2008; Widom, 1995) and thermodynamics of their nucleation (see, e.g., Gretz, 1966a,b; Iwamatsu, 2015a,b; Navascués and Tarazona, 1981; Scheludko, 1980, 1983, 1985; Singha et al., 2015). However, many of them may be "theoretical artifacts" due to extrapolation of simple macroscopic equations down to submicrometer and nanosized droplets.

In our consideration, we have neglected dependence of the liquid–vapor surface tension $\sigma^{\alpha\beta}$ on the chemical potential. Constancy of $\sigma^{\alpha\beta}$ is a part of the employed ID model; however, within general thermodynamic treatment it can be taken into account by using the most general equation (11), which can be rewritten as

$$\sigma_0^{\alpha\beta}(\cos\theta_0 - \cos\theta) = \delta\Delta\sigma^\gamma + \delta\sigma^{\alpha\beta}\cos\theta + \kappa/r + \partial\kappa/\partial r \quad \text{with} \quad \delta\sigma^{\alpha\beta} \equiv \sigma^{\alpha\beta} - \sigma_0^{\alpha\beta}, \tag{58}$$

extracting $\delta\sigma^{\alpha\beta}\cos\theta \simeq \delta\sigma^{\alpha\beta}\cos\theta_0$ as an additional correction term. Since Eqs. (8), (9) and, therefore, (11) are obtained using the surface of tension as the $\alpha\beta$ dividing surface, $\partial\sigma^{\alpha\beta}/\partial R = 0$, and the Gibbs adsorption equation takes the form $\mathrm{d}\sigma^{\alpha\beta} = -\Gamma^{\alpha\beta}\,\mathrm{d}\mu$. Then, $\delta\sigma^{\alpha\beta} \simeq -\Gamma_0^{\alpha\beta}\delta\mu$, and, for the slope of the curve $\cos\theta$ vs. $1/r$, with account of correction due to adsorption at $\alpha\beta$ interface, we obtain

$$-\kappa_0/\sigma_0^{\alpha\beta} - 2\sin\theta_0\left(\Gamma_0^{\beta\gamma} - \Gamma_0^{\alpha\gamma} - \Gamma_0^{\alpha\beta}\cos\theta_0\right)/n^\alpha \tag{59}$$

instead of (24). While, in general, an additional correction $2\Gamma_0^{\alpha\beta}\sin\theta_0\cos\theta_0/n^\alpha$ may be significant for very small sessile droplets, in the considered case of nucleation with initial formation of a polymolecular precursor film, it is not

significant, since f_0 is usually much larger than the Tolman length. In any case, it seems reasonable to consider this effect together with higher-order corrections, such as droplet-size dependence of $\delta\Delta\sigma^{\gamma}$, κ and $\partial\kappa/\partial r$.

In a recent work of Kanduč (2017), size-dependence of the contact angle was studied by molecular-dynamics simulations for nanosized cylindrical (ridge-shaped) sessile water droplets. In such geometry, the term κ/r is absent in the generalized Young Eq. (9) and in Eq. (11), while the term $\partial\kappa/\partial r$ persists and thus its effect on the contact angle can be studied separately.** Kanduč (2017) has attributed this effect to the contact-angle dependence of the line tension, using the "line-tension stiffness" $\partial\kappa/\partial\theta$ that can be understood as $(\partial\kappa/\partial r)(\partial r/\partial\theta)_R = (\partial\kappa/\partial r)R\cos\theta$. Its effect was studied together with effect of curvature-dependence $\sigma^{\alpha\beta}(R)$ of the liquid–vapor surface tension taking into account a linear in $1/R$ correction with use of the Tolman length. The solid–fluid-adsorption-related change of $\Delta\sigma^{\gamma}$ was not considered. It was found that the line-tension-stiffness correction to the contact angle is significant or even predominant for polar substrates and negligible for non-polar ones. In contrast to our results, dependences of $\cos\theta$ vs. $1/R$ (and, therefore $1/r$) have been found linear even for very small values of R (such as a few nanometers).

ACKNOWLEDGMENTS

The work was supported by the Russian Foundation for Basic Research (grant no. 16-03-01140-a).

REFERENCES

Ajaev, V.S., Instability and rupture of thin liquid films on solid substrates, *Interf. Phenom. Heat Transf.*, vol. **1**, no. 1, pp. 81–92, 2013.

Amirfazli, A., Kwok, D., Gaydos, J., and Neumann, A., Line tension measurements through drop size dependence of contact angle, *J. Colloid Interf. Sci.*, vol. **205**, no. 1, pp. 1–11, 1998.

Blossey, R. and Bausch, R., Dynamics of first-order wetting transitions, *Phase Trans.*, vol. **50**, no. 1–3, pp. 113–122, 1994.

Bykov, T.V. and Shchekin, A.K., Surface tension, Tolman length, and effective rigidity constant in the surface layer of a drop with a large radius of curvature, *Inorganic Materials*, vol. **35**, no. 6, pp. 641–644, 1999a.

Bykov, T.V. and Shchekin, A.K., Thermodynamic characteristics of a small droplet in terms of the density functional method, *Colloid J.*, vol. **61**, no. 2, pp. 144–151, 1999b.

Checco, A., Guenoun, P., and Daillant, J., Nonlinear dependence of the contact angle of nanodroplets on contact line curvature, *Phys. Rev. Lett.*, vol. **91**, no. 18, p. 186101, 2003.

Churaev, N.V., Starov, V.M., and Derjaguin, B.V., The shape of the transition zone between a thin film and bulk liquid and the line tension, *J. Colloid Interf. Sci.*, vol. **89**, no. 1, pp. 16–24, 1982.

Dash, J.G., Clustering and percolation transitions in helium and other thin films, *Phys. Rev. B*, vol. **15**, no. 6, pp. 3136–3146, 1977.

de Gennes, P.G., Wetting: statics and dynamics, *Rev. Mod. Phys.*, vol. **57**, no. 3, pp. 827–863, 1985.

Derjaguin, B.V., Churaev, N.V., and Muller, V.M., *Surface Forces*, Consultants Bureau, Plenum Press, New York, 1987.

Derjaguin, B.V. and Zorin, Z.M., Issledovaniya poverkhnostnoy kondensatsii i adsorbtsii parov vblizi nasyscheniya opticheskim mikropolyarizatsionnym metodom. II., *Zh. Fiz. Khim.*, vol. **29**, no. 10, pp. 1755–1770, 1955.

Dietrich, S., 1988. Wetting phenomena, *Phase Transitions and Critical Phenomena*. Domb, C. and Lebowitz, J.L. (Eds.). Vol. 12. Academic Press, Ch. 1, pp. 1–218.

Dobbs, H., The modified Young's equation for the contact angle of a small sessile drop from an interface displacement model, *Int. J. Mod. Phys. B*, vol. **13**, no. 27, pp. 3255–3259, 1999.

Dobbs, H.T. and Indekeu, J.O., Line tension at wetting: interface displacement model beyond the gradient-squared approximation, *Physica A*, vol. **201**, no. 4, pp. 457–481, 1993.

Fletcher, N.H., Size effect in heterogeneous nucleation, *The Journal of Chemical Physics*, vol. **29**, no. 3, pp. 572–576, 1958.

Getta, T. and Dietrich, S., Line tension between fluid phases and a substrate, *Phys. Rev. E*, vol. **57**, no. 1, pp. 655–671, 1998.

Gretz, R.D., Line-tension effect in a surface energy model of a capshaped condensed phase, *J. Chem. Phys.*, vol. **45**, no. 8, pp. 3160–3161, 1966a.

**Size-dependence of the line tension here differs from the one for spherical-segment-shaped droplets for the same substances.

Gretz, R.D., The line-tension effect in heterogeneous nucleation, *Surf. Sci.*, vol. **5**, no. 2, pp. 239–251, 1966b.

Herminghaus, S., Pompe, T., and Fery, A., Scanning force microscopy investigation of liquid structures and its application to fundamental wetting research, *J. Adhesion Sci. Technol.*, vol. **14**, no. 14, pp. 1767–1782, 2000.

Indekeu, J.O., Line tension near the wetting transition: results from an interface displacement model, *Physica A*, vol. **183**, no. 4, pp. 439–461, 1992.

Indekeu, J.O. and Bonn, D., Nucleation and wetting near surface spinodals, *Phys. Rev. Lett.*, vol. **74**, no. 19, pp. 3844–3847, 1995.

Indekeu, J.O. and Bonn, D., The role of surface spinodals in nucleation and wetting phenomena, *J. Mol. Liquids*, vol. **71**, no. 2, pp. 163–173, 1997.

Iwamatsu, M., Line-tension effects on heterogeneous nucleation on a spherical substrate and in a spherical cavity, *Langmuir*, vol. **31**, no. 13, pp. 3861–3868, 2015a.

Iwamatsu, M., Line-tension-induced scenario of heterogeneous nucleation on a spherical substrate and in a spherical cavity, *J. Chem. Phys.*, vol. **143**, no. 1, p. 014701, 2015b.

Kanduč, M., Going beyond the standard line tension: Size-dependent contact angles of water nanodroplets, *J. Chem. Phys.*, vol. **147**, no. 17, p. 174701, 2017.

Kuni, F.M., Shchekin, A.K., and Grinin, A.P., Theory of heterogeneous nucleation for vapor undergoing a gradual metastable state formation, *Physics-Uspekhi*, vol. **44**, no. 4, pp. 331–370, 2001.

Kuni, F.M., Shchekin, A.K., Rusanov, A.I., and Widom, B., Role of surface forces in heterogeneous nucleation on wettable nuclei, *Adv. Colloid Interf. Sci.*, vol. **65**, pp. 71–124, 1996.

Law, B.M., McBride, S.P., Wang, J.Y., Wi, H.S., Paneru, G., Betelu, S., Ushijima, B., Takata, Y., Flanders, B., Bresme, F., Matsubara, H., Takiue, T., and Aratono, M., Line tension and its influence on droplets and particles at surfaces, *Progr. Surf. Sci.*, vol. **92**, no. 1, pp. 1–39, 2017.

Lv, C., Yin, Y., and Zheng, Q., Nonlinear effects of line tension in adhesion of small droplets, *Appl. Math. Mech.-Engl. Ed.*, vol. **29**, no. 10, pp. 1251–1262, 2008.

Marmur, A., Line tension effect on contact angles: Axisymmetric and cylindrical systems with rough or heterogeneous solid surfaces, *Colloids Surf. A*, vol. **136**, no. 1, pp. 81–88, 1998.

Mechkov, S., Oshanin, G., Rauscher, M., Brinkmann, M., Cazabat, A.M., and Dietrich, S., Contact line stability of ridges and drops, *Europhys. Lett.*, vol. **80**, no. 6, p. 66002, 2007.

Nakanishi, H. and Pincus, P., Surface spinodals and extended wetting in fluids and polymer solutions, *J. Chem. Phys.*, vol. **79**, no. 2, pp. 997–1003, 1983.

Navascués, G. and Tarazona, P., Line tension effects in heterogeneous nucleation theory, *J. Chem. Phys.*, vol. **75**, no. 5, pp. 2441–2446, 1981.

Radoev, B., Scheludko, A., and Toshev, B.V., On the energetics of new phase formation, *J. Colloid Interf. Sci.*, vol. **113**, no. 1, pp. 1–4, 1986.

Rusanov, A.I., On the wetting theory of elastically deformable bodies. 5. Reducing the deformation effects to linear tension, *Colloid J. USSR*, vol. **39**, p. 618, 1977.

Rusanov, A.I., On the thermodynamics of deformable solid surfaces, *J. Colloid Interface Sci.*, vol. **63**, no. 2, pp. 330–345, 1978.

Rusanov, A.I., Thermodynamics of solid surfaces, *Surf. Sci. Rep.*, vol. **23**, no. 6–8, pp. 173–247, 1996.

Rusanov, A.I., Surface thermodynamics revisited, *Surf. Sci. Rep.*, vol. **58**, no. 5–8, pp. 111–239, 2005.

Rusanov, A.I., Shchekin, A.K., and Tatyanenko, D.V., The line tension and the generalized young equation: the choice of dividing surface, *Colloids Surf. A*, vol. **250**, no. 1–3, pp. 263–268, 2004.

Rusanov, A.I., Shchekin, A.K., and Tatyanenko, D.V., Grand potential in thermodynamics of solid bodies and surfaces, *J. Chem. Phys.*, vol. **131**, no. 16, p. 161104, 2009.

Rusanov, A.I., Tatyanenko, D.V., and Shchekin, A.K., New approach to defining thermodynamic surface tension of solids, *Colloid J.*, vol. **72**, no. 5, pp. 673–678, 2010.

Scheludko, A., On the role of line tension in heterogeneous phase formation, *Colloids Surf.*, vol. **1**, no. 2, pp. 191–196, 1980.

Scheludko, A., On the theory of heterogeneous phase formation, *Colloids Surf.*, vol. **7**, no. 1, pp. 81–86, 1983.

Scheludko, A.D., Condensation of vapors on spherical nuclei and the line tension effect, *J. Colloid Interf. Sci.*, vol. **104**, no. 2, pp.

471–476, 1985.

Seemann, R., Jacobs, K., and Blossey, R., Polystyrene nanodroplets, *J. Phys.: Condens. Matter*, vol. **13**, no. 21, p. 4915, 2001.

Singha, S.K., Das, P.K., and Maiti, B., Inclusion of line tension effect in classical nucleation theory for heterogeneous nucleation: A rigorous thermodynamic formulation and some unique conclusions, *J. Chem. Phys.*, vol. **142**, no. 10, p. 104706, 2015.

Volmer, M., *Kinetik der Phasenbildung*, Th. Steinkopff, Dresden, 1939.

Ward, C.A. and Wu, J., Effect of contact line curvature on solid–fluid surface tensions without line tension, *Phys. Rev. Lett.*, vol. **100**, no. 25, p. 256103, 2008.

Warshavsky, V.B., Podguzova, T.S., Tatyanenko, D.V., and Shchekin, A.K., Thermodynamics of a liquid wetting film on a spherical particle with an adsorbed ion, *Colloid J.*, vol. **75**, no. 5, pp. 504–513, 2013a.

Warshavsky, V.B., Podguzova, T.S., Tatyanenko, D.V., and Shchekin, A.K., Vapor nucleation on a wettable nanoparticle carrying a non-central discrete electric charge, *J. Chem. Phys.*, vol. **138**, no. 19, p. 194708, 2013b.

Widom, B., Line tension and the shape of a sessile drop, *J. Phys. Chem.*, vol. **99**, no. 9, pp. 2803–2806, 1995.